OPEN

Diagnostic Ultrasound and Microbubbles Treatment Improves Outcomes of Coronary No-Reflow in Canine Models by Sonothrombolysis

Hairui Li, MD, PhD[1]; Yongkang Lu, MD, PhD[2]; Yili Sun, MD[1]; Gangbin Chen, MD[3]; Junfen Wang, MD, PhD[4]; Shifei Wang, MD, PhD[1]; Chixiong Huang, MD[1]; Lintao Zhong, MD, PhD[1]; Xiaoyun Si, MD, PhD[1]; Wangjun Liao, MD, PhD[5]; Yulin Liao, MD, PhD[1]; Shiping Cao, MD, PhD[1]; Jianping Bin, MD, PhD[1]

Objectives: Effective treatment for microvascular thrombosis-induced coronary no-reflow remains an unmet clinical need. This study sought to evaluate whether diagnostic ultrasound and microbubbles treatment could improve outcomes of coronary no-reflow by dissolving platelet- and erythrocyte-rich microthrombi.

Design: Randomized controlled laboratory investigation.

Setting: Research laboratory.

Subjects: Mongrel dogs.

Interventions: Coronary no-reflow models induced by platelet- or erythrocyte-rich microthrombi were established and randomly assigned to control, ultrasound, recombinant tissue-type plasminogen activator, ultrasound + microbubbles, or ultrasound + microbubbles + recombinant tissue-type plasminogen activator group. All treatments lasted for 30 minutes.

Measurements and Main Results: Percentage of microemboli-obstructed coronary arterioles was lower in ultrasound + microbubbles group than that in control group for platelet- (> 50% obstruction: 10.20% ± 3.56% vs 31.80% ± 3.96%; < 50% obstruction: 14.80% ± 4.15% vs 28.20% ± 3.56%) and erythrocyte-rich microthrombi (> 50% obstruction: 8.20% ± 3.11% vs 30.60% ± 4.83%; < 50% obstruction: 12.80% ± 4.15% vs 25.80% ± 3.70%) ($p < 0.001$). Percentage change of myocardial blood flow in left anterior descending artery-dominated region, left ventricular ejection fraction, fractional shortening, and ST-segment resolution were higher, whereas infarcted area, troponin I, and creatine kinase MB isoenzyme were lower in ultrasound + microbubbles group than that in control group for both types of microthrombi ($p < 0.001$). Percentage change of myocardial blood flow, ejection fraction, fractional shortening, and ST-segment resolution were higher, whereas infarcted area, troponin I, and creatine kinase MB isoenzyme were lower in ultrasound + microbubbles and ultrasound + microbubbles + recombinant tissue-type plasminogen activator groups than that in recombinant tissue-type plasminogen activator group for platelet-rich microthrombi ($p < 0.05$).

Conclusions: Ultrasound + microbubbles treatment could dissolve platelet- and erythrocyte-rich microthrombi, thereby improving outcomes of coronary no-reflow, making it a promising supplement to current reperfusion therapy for acute ST-segment elevation myocardial infarction. (*Crit Care Med* 2018; 46:e912–e920)

Key Words: coronary no-reflow; diagnostic ultrasound; erythrocyte-rich microthrombi; microbubbles; myocardial infarction; platelet-rich microthrombi

[1]State Key Laboratory of Organ Failure Research, Department of Cardiology, Nanfang Hospital, Southern Medical University, Guangzhou, China.

[2]Department of Cardiac Internal Medicine, Shenzhen Sun Yat-Sen Cardiovascular Hospital, Shenzhen, China.

[3]Department of Cardiology, Shantou Central Hospital, Shantou, China.

[4]Department of Gastroenterology, Guangdong Provincial Key Laboratory of Gastroenterology, Nanfang Hospital, Southern Medical University, Guangzhou, China.

[5]Department of Oncology, Nanfang Hospital, Southern Medical University, Guangzhou, China.

The animal experiments were performed at the State Key Laboratory of Organ Failure Research, Nanfang Hospital, Southern Medical University.

Supplemental digital content is available for this article. Direct URL citations appear in the printed text and are provided in the HTML and PDF versions of this article on the journal's website (http://journals.lww.com/ccmjournal).

Supported, in part, by grants from the National Natural Science Foundation of China (81571698, 81227801, and 81271640), National Basic Research Program of China (973 Program) (2013CB733804), and the Team Program of Natural Science Foundation of Guangdong Province, China (S2011030003134) (to Dr. Bin), and from the National Natural Science Foundation of China (81471679) (to Dr. Cao).

Dr. S. Wang disclosed government work. The remaining authors have disclosed that they do not have any potential conflicts of interest.

For information regarding this article, E-mail: jianpingbin@hotmail.com; jianpingbin@126.com; csp2012@126.com

DOI: 10.1097/CCM.0000000000003255

Despite timely reperfusion intervention, coronary no-reflow (CnRF) still occurs in more than a third of ST-segment elevation myocardial infarction (STEMI) patients, resulting in poor clinical outcomes (1). Microvascular thrombosis or spasm, neutrophilic plugging, and/or tissue edema have been shown to be responsible for CnRF, among which microvascular thrombosis is considered to be crucial (2). Both platelet-rich microthrombi (PRT) and erythrocyte-rich microthrombi (ERT) (3), due to distal dislodgement of upstream thrombotic debris (4) or ischemia-reperfusion injury–induced intravascular microthrombosis (5), contribute to the thrombosed coronary microvessels.

Current clinical preventions or therapies for microvascular thrombotic occlusion are lacking in effectiveness and safety. Thrombolytics may effectively lyse ERT, but the heightened risk of fatal bleeding and futility in dissolving PRT has limited their use in the clinic (6). An additional glycoprotein IIb/IIIa inhibitor on the basis of current routine double antiplatelet therapy before percutaneous coronary intervention is theoretically potent in suppressing microthrombi formation (7). However, evidence regarding their utility in reducing CnRF is controversial, and the European Society of Cardiology/European Association for Cardio-Thoracic Surgery guideline (2014) recommends their use only for bailout procedures (8). Other treatments, such as the placement of distal protection devices and thrombus aspiration, were successful in experimental and small capacity clinical studies (9) but failed to improve outcomes in STEMI patients in large clinical trials (10). Recently, a novel therapy, sphingosine-1-phosphate receptor agonist, has been successfully administered before reperfusion to prevent reperfusion injury; however, there is no therapy that is currently useful for posttherapy (11).

Diagnostic ultrasound (US) combined with microbubbles (MBs) can be not only used for the detection of myocardium at risk of ischemia (12) and thrombus (13–15) but also used for dissolving thrombus. A wealth of studies have demonstrated the tremendous effectiveness of US+MB treatment in lysing macrothrombi occluding the epicardial coronary, large cerebral, and peripheral arteries (16–18). Recently, our team and others demonstrated that this treatment was highly effective in dissolving microthrombi (platelet- and erythrocyte-rich) in vitro (19), in vivo (20, 21), and alleviating brain injury in thrombotic microembolism-induced acute ischemic stroke (22). Furthermore, several studies have determined that US+MB treatment could improve microvascular perfusion in models of acute myocardial infarction (MI) (18, 23, 24) and ischemia-reperfusion injury (25). In those studies, two potential mechanisms, nitric oxide release and dissolution of microthrombi, were proposed to be responsible for the improvement of microvascular perfusion after receiving US+MB treatment. However, whether the improvement of coronary microvascular perfusion by US+MB treatment was resulted from the dissolution of microthrombi has not been determined. In addition, the efficacy of US+MB treatment in lysing erythrocyte-rich or PRT, particularly for PRT, which is responsible for the largest proportion of CnRF patients, has not been directly evaluated.

We hypothesize that US+MB treatment could improve the outcomes of CnRF by dissolving both PRT and ERT. To verify our hypothesis, an in vitro setup simulating coronary microembolization and a rat model of mesenteric arteriolar microthrombosis was established to investigate the lytic efficacy of US+MB treatment on both PRT and ERT. More importantly, the efficacy and safety of this treatment in dissolving both types of microthrombi and improving the outcomes were assessed in a canine CnRF model.

METHODS

The study was reviewed and approved by Institutional Review Board of Southern Medical University. CnRF models induced by PRT or ERT were established and randomly assigned to control (CON), US, recombinant tissue-type plasminogen activator (rtPA), US+MB, or US+MB+rtPA group. All treatments lasted for 30 minutes. Myocardial contrast echocardiography (MCE)-derived myocardial blood flow (MBF), ST-segment resolution (STR), and M-mode US-determined cardiac systolic functions were assessed both before and 6 hours after treatment. The hearts were harvested, and venous blood was drawn 6 hours after treatment. 2,3,5-triphenyl-2H-tetrazolium chloride (TTC)-derived infarcted volume, transferase-mediated deoxyuridine triphosphate-biotin nick end labeling (TUNEL)-determined apoptotic cardiomyocyte, and enzyme-linked immunosorbent assay (ELISA)-measured cardiac markers were analyzed. All methods are described in detail in the **supplemental methods** (Supplemental Digital Content 1, http://links.lww.com/CCM/D697).

RESULTS

Histopathologic Characterization and Contrast-Enhanced US Imaging of Macrothrombi

Hematoxylin & eosin (HE) staining and scanning electronic microscopy (SEM) both demonstrated that platelet-rich macrothrombi composed of dense fibrin-platelet networks and a few erythrocytes, whereas ERT composed of clustered erythrocytes. In addition, freshly prepared platelet-rich macrothrombi had a relatively loose structure and more microchannels than erythrocyte-rich macrothrombi. As macrothrombi increased in age, both types became denser with fewer microchannels, particularly in platelet-rich macrothrombi (**Fig. S2, *A* and *B***, Supplemental Digital Content 3, http://links.lww.com/CCM/D699).

The video intensity (VI) was higher in freshly prepared platelet-rich macrothrombi (5.15 ± 0.19) compared with freshly prepared erythrocyte-rich macrothrombi (4.96 ± 0.25) but was lower in older platelet-rich macrothrombi (0.29 ± 0.16) compared with erythrocyte-rich macrothrombi (1.03 ± 0.21) ($n = 8$; $p < 0.001$) (**Fig. S2, *C* and *G***, Supplemental Digital Content 3, http://links.lww.com/CCM/D699).

In Vitro Thrombolytic Efficacy of US+MB Treatment

The decrease in pressure was greater in US+MB (PRT: 77.81% ± 3.64%; ERT: 78.75% ± 2.99%) and US+MB+rtPA groups (PRT: 79.69% ± 3.64%; ERT: 91.56% ± 3.52%) than that in

CON group (PRT: 5.63% ± 3.20%; ERT: 6.25% ± 2.99%) but was similar in US and CON groups for both the PRT and ERT. The decrease in pressure upstream of the mesh was significantly lower after treatment in rtPA group (41.88% ± 5.30%) than that in the US+MB group (77.81% ± 3.64%) but was similar in US+MB and US+MB+rtPA groups (79.68% ± 3.64%) for PRT. Conversely, the decrease in pressure was similar after treatment in rtPA (76.25% ± 3.54%) and US+MB groups, but significantly higher in US+MB+rtPA group for ERT ($n = 8$; $p < 0.001$) (**Fig. S2*E***, Supplemental Digital Content 3, http://links.lww.com/CCM/D699).

The decrease in pressure was comparable between the freshly prepared PRT (76.25% ± 2.99%) and ERT groups (77.81% ± 3.64%) after treatment. However, the decrease in pressure was greater in older ERT (38.13% ± 3.72%) than that in older PRT group (19.38% ± 2.59%) ($n = 8$; $p < 0.001$) (**Fig. S2*F***, Supplemental Digital Content 3, http://links.lww.com/CCM/D699).

Effectiveness of US+MB Treatment on Mesenteric Microthrombi

Rat mesenteric microthrombosis models, induced by both PRT and ERT, were successfully established. HE staining demonstrated that PRT composed of dense fibrin-platelet networks and a few erythrocytes, whereas ERT were mainly composed of clustered RBCs. The freshly prepared PRT had a relatively loose structure and more microchannels than erythrocyte-rich ones. As the age of microthrombi increased, both types of microthrombi became denser with fewer microchannels, particularly for PRT. Transmission electronic microscopy showed that the PRT were abundant in platelets, whereas the ERT were abundant in erythrocytes (**Fig. S3, *A* and *B***, Supplemental Digital Content 4, http://links.lww.com/CCM/D700).

No spontaneous dissolution of PRT and ERT occurred in the CON group. Both types of microthrombi were successfully lysed, blood flow within the mesenteric arterioles was restored, and no reocclusion occurred within 30 minutes after treatment in US+MB group (**Fig. S3, *C* and *D***, Supplemental Digital Content 4, http://links.lww.com/CCM/D700), as shown by the intravital microscope. For both types of microthrombi, the recanalization rate in US+MB (PRT: 75% vs 0%; ERT: 83% vs 0%) and US+MB+rtPA groups (PRT: 83% vs 0%; ERT: 100% vs 0%) was significantly higher than that in CON groups ($n = 12$; $p < 0.001$) (**Fig. S3*E***, Supplemental Digital Content 4, http://links.lww.com/CCM/D700). For ERT, the recanalization rate was higher in rtPA group (33%) than that in CON group (0%) after treatment ($n = 12$; $p = 0.001$) (Fig. S3*E*, Supplemental Digital Content 4, http://links.lww.com/CCM/D700).

US+MB Treatment Lysed Microthrombi in the Coronary Microvasculature

Diameters of microthrombi prepared in vitro ranged from 70 to 100 μm, similar to those found in the embolized coronary microvasculature. Both HE staining and SEM demonstrated that PRT composed of dense fibrin-platelet meshworks and a few erythrocytes, whereas ERT consisted of a compact mass of erythrocytes and a relatively loose fibrin network (**Fig. S1**, Supplemental Digital Content 2, http://links.lww.com/CCM/D698).

HE and immunohistochemical staining showed that myocardial arterioles were obstructed by PRT or ERT, containing platelets (CD41) and fibrin (fibrinogen) (**Figs. 1** and **2**). For both types of microthrombi, the percentage of myocardial arterioles occluded by microthrombi was lower in US+MB group compared with CON group (PRT: > 50% obstruction: 10.20% ± 3.56% vs 31.80% ± 3.96%, < 50% obstruction: 14.80% ± 4.15% vs 28.20% ± 3.56%; ERT: > 50% obstruction: 8.20% ± 3.11% vs 30.60% ± 4.83%, < 50% obstruction: 12.80% ± 4.15% vs 25.80% ± 3.70%) ($n = 5$; $p \leq 0.001$) (**Fig. 3*A***). In addition, HE staining showed no perivascular hemorrhage (**Fig. S9*C***, Supplemental Digital Content 10, http://links.lww.com/CCM/D706).

US+MB Treatment Improved Myocardial Perfusion

As shown in **Figure S5** (Supplemental Digital Content 6, http://links.lww.com/CCM/D702) and **Figure S6** (Supplemental Digital Content 7, http://links.lww.com/CCM/D703), the differences in baseline parameters, including VI, β value (transit rate), MBF, and STR, between groups were statistically insignificant. For both types of microthrombi, the increases (times) in VI (PRT: 1.97 ± 0.13 vs 0.20 ± 0.09, 2.09 ± 0.16 vs 0.20 ± 0.09; ERT: 2.04 ± 0.15 vs 0.20 ± 0.11, 2.45 ± 0.15 vs 0.20 ± 0.11; $n = 5$; $p < 0.001$), β value (PRT:

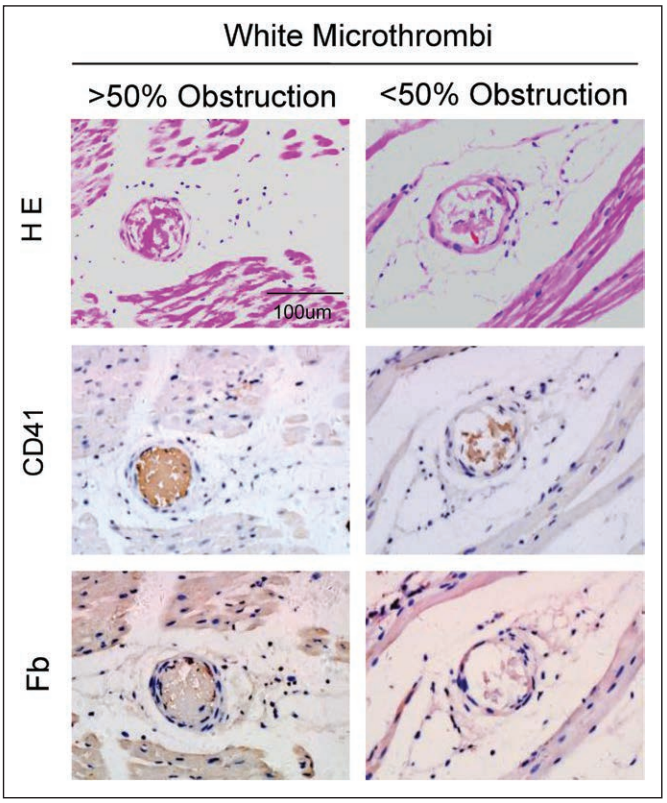

Figure 1. Histopathologic examination of coronary microthrombi. Representative images of platelet-rich microthrombi in coronary arterioles as shown by hematoxylin & eosin (HE) or immunohistochemical staining (anti-CD41 and antifibrinogen [anti-Fb] antibodies).

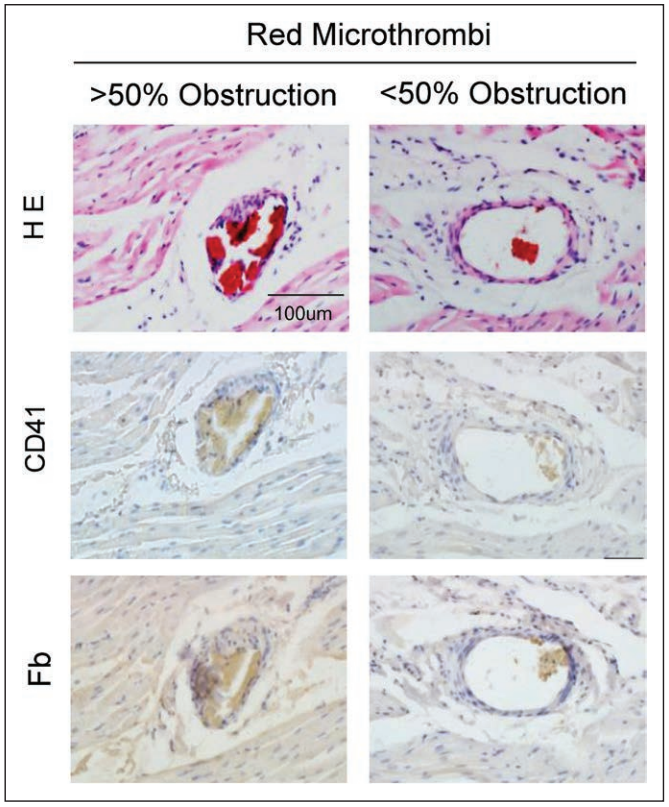

Figure 2. Histopathologic examination of coronary microthrombi. Representative images of erythrocyte-rich microthrombi in coronary arterioles as shown by hematoxylin & eosin (HE) or immunohistochemical staining (anti-CD41 and antifibrinogen [anti-Fb] antibodies).

0.47 ± 0.10 vs 0.09 ± 0.06, 0.47 ± 0.12 vs 0.09 ± 0.06; ERT: 0.47 ± 0.10 vs 0.12 ± 0.09, 0.69 ± 0. 09 vs 0.12 ± 0.09; $p < 0.001$) (**Fig. S7**, Supplemental Digital Content 8, http://links.lww.com/CCM/D704; **Fig. S8**, Supplemental Digital Content 9, http://links.lww.com/CCM/D705), and MBF (PRT: 3.38 ± 0.40 vs 0.37 ± 0.12, 3.55 ± 0.42 vs 0.37 ± 0.12; ERT: 3.46 ± 0.45 vs 0.34 ± 0.21, 4.83 ± 0.54 vs 0.34 ± 0.21; $p < 0.001$) (**Fig. 3, *B* and *C***) in US+MB and US+MB+rtPA groups were higher than those in CON group, but were similar in CON and US groups (Fig. S7, Supplemental Digital Content 8, http://links.lww.com/CCM/D704; Fig. S8, Supplemental Digital Content 9, http://links.lww.com/CCM/D705). Similarly, the STR (times) (PRT: 0.61 ± 0.05 vs 0.18 ± 0.02, 0.68 ± 0.07 vs 0.18 ± 0.02; ERT: 0.61 ± 0.07 vs 0.17 ± 0.03, 0.80 ± 0.06 vs 0.17 ± 0.03; $n = 5$; $p < 0.001$) was greater in US+MB and US+MB+rtPA groups than that in CON group (**Fig. 4, *A* and *B***). For PRT, the increases of VI (1.97 ± 0.13 vs 1.10 ± 0.15; $p < 0.001$), β value (0.47 ± 0.10 vs 0.29 ± 0.04; $p = 0.021$) (Fig. S7, Supplemental Digital Content 8, http://links.lww.com/CCM/D704), MBF (3.38 ± 0.40 vs 1.70 ± 0.20; $p < 0.001$) (Fig. 3, *B* and *C*), and STR (0.61 ± 0.05 vs 0.42 ± 0.05; $p < 0.001$) (Fig. 4, *A* and *B*) in US+MB group after treatment were significantly higher than those in rtPA group and were comparable between US+MB and US+MB+rtPA groups. For ERT, the increases in VI value (2.45 ± 0.15 vs 2.03 ± 0.14, 2.45 ± 0.15 vs 2.04 ± 0.15; $n = 5$; $p = 0.001$), β value (0.69 ± 0.09 vs 0.49 ± 0.08, $p = 0.016$; 0.69 ± 0.09 vs 0.47 ± 0.10, $p = 0.006$) (Fig. S8, Supplemental Digital Content 9, http://links.lww.com/CCM/D705), MBF (4.83 ± 0.54 vs 3.51 ± 0.40, $p = 0.021$; 4.83 ± 0.54 vs 3.46 ± 0.45, $p = 0.020$) (Fig. 3, *B* and *C*), and STR (0.80 ± 0.06 vs 0.61 ± 0.06, 0.80 ± 0.06 vs 0.61 ± 0.07; $p < 0.001$) (Fig. 4, *A* and *B*) were higher in US+MB+rtPA group, but similar in rtPA and US+MB groups ($n = 5$). In addition, the occurrence rate of premature ventricular contractions was nonsignificant among CON, US, and US+MB groups (**Fig. S9*D***, Supplemental Digital Content 10, http://links.lww.com/CCM/D706).

US+MB Treatment Reduced Myocardial Injury

For both types of microthrombi, the TTC-defined necrotic area (PRT: 12.72% ± 2.14% vs 35.33% ± 3.10%, 12.57% ± 2.04% vs 35.33% ± 3.10%; ERT: 12.52% ± 1.87% vs 34.91% ± 3.39%, 5.96% ± 1.12% vs 34.91% ± 3.39%; $n = 5$; $p < 0.001$) was smaller in US+MB and US+MB+rtPA groups than in CON group, but was similar in CON and US groups (**Fig. 4**, ***C*** and ***D***; **Fig. S9, *A* and *B***, Supplemental Digital Content 10, http://links.lww.com/CCM/D706). Similarly, creatine kinase MB isoenzyme (PRT: 1.54 ± 0.19 × 10^3 U/mL vs 2.64 ± 0.21 × 10^3 U/mL, 1.51 ± 0.21 × 10^3 U/mL vs 2.64 ± 0.21 × 10^3 U/mL; ERT: 1.53 ± 0.15 × 10^3 U/mL vs 2.62 ± 0.21 × 10^3 U/mL, 1.03 ± 0.15 × 10^3 U/mL vs 2.62 ± 0.21 × 10^3 U/mL; $n = 5$; $p < 0.001$) and troponin I (TnI) (PRT: 0.37 ± 0.04 ng/mL vs 1.16 ± 0.09 ng/mL, 0.36 ± 0.05 ng/mL vs 1.16 ± 0.09 ng/mL; ERT: 0.37 ± 0.04 ng/mL vs 1.14 ± 0.09 ng/mL, 0.13 ± 0.02 ng/mL vs 1.14 ± 0.09 ng/mL; $p < 0.001$) were lower in US+MB and US+MB+rtPA groups than in CON group (**Fig. 5*A***). For PRT, the necrotic area (12.72% ± 2.14% vs 24.13% ± 2.89%; $p < 0.001$) (Fig. 4, *C* and *D*; Fig. S9*A*, Supplemental Digital Content 10, http://links.lww.com/CCM/D706), CK-MB (1.54 ± 0.19 × 10^3 U/mL vs 2.07 ± 0.22 × 10^3 U/mL; $p = 0.008$) and TnI (0.37 ± 0.04 ng/mL vs 0.61 ± 0.07 ng/mL; $p < 0.001$) (Fig. 5*A*) were lower in US+MB group than in rtPA group and were comparable between US+MB and US+MB+rtPA groups. For ERT, the necrotic area (5.96% ± 1.12% vs 14.13% ± 2.94%, $p = 0.001$; 5.96% ± 1.12% vs 12.52% ± 1.87%, $p = 0.006$) (Fig. 4, *C* and *D*; Fig. S9*B*, Supplemental Digital Content 10, http://links.lww.com/CCM/D706), CK-MB (1.03 ± 0.15 × 10^3 U/mL vs 1.55 ± 0.15 × 10^3 U/mL, 1.03 ± 0.15 × 10^3 U/mL vs 1.53 ± 0.15 × 10^3 U/mL; $p = 0.002$), and TnI (0.13 ± 0.02 ng/mL vs 0.37 ± 0.04 ng/mL, 0.13 ± 0.02 ng/mL vs 0.37 ± 0.04 ng/mL; $p < 0.001$) (Fig. 5*A*) were lower in US+MB+rtPA group, but similar in rtPA and US+MB groups.

US+MB Treatment Improved Cardiac Functions

For both types of microthrombi, the percentage increases in ejection fraction (EF) (PRT: 9.16% ± 0.61% vs 1.44% ± 1.31%, 9.60% ± 1.62% vs 1.44% ± 1.31%; ERT: 8.98% ± 0.96% vs 1.96% ± 1.10%, 12.08% ± 1.16% vs 1.96% ± 1.10%) and fractional shortening (FS) (PRT: 17.10% ± 1.70% vs 2.81% ± 2.57%, 18.52% ± 3.03% vs 2.81% ± 2.57%; ERT 18.04% ± 0.69% vs 3.86% ± 2.17%, 23.66% ± 2.15% vs 3.86% ± 2.17%) in US+MB and US+MB+rtPA groups were greater than those in CON group ($n = 5$; $p < 0.001$) and were similar in CON and US groups (**Fig. 5*B***). For PRT, the percentage increases in EF (9.16% ± 0.61% vs 5.24% ± 1.04%; $p < 0.001$) and FS (17.10% ± 1.70% vs 10.80% ± 2.34%;

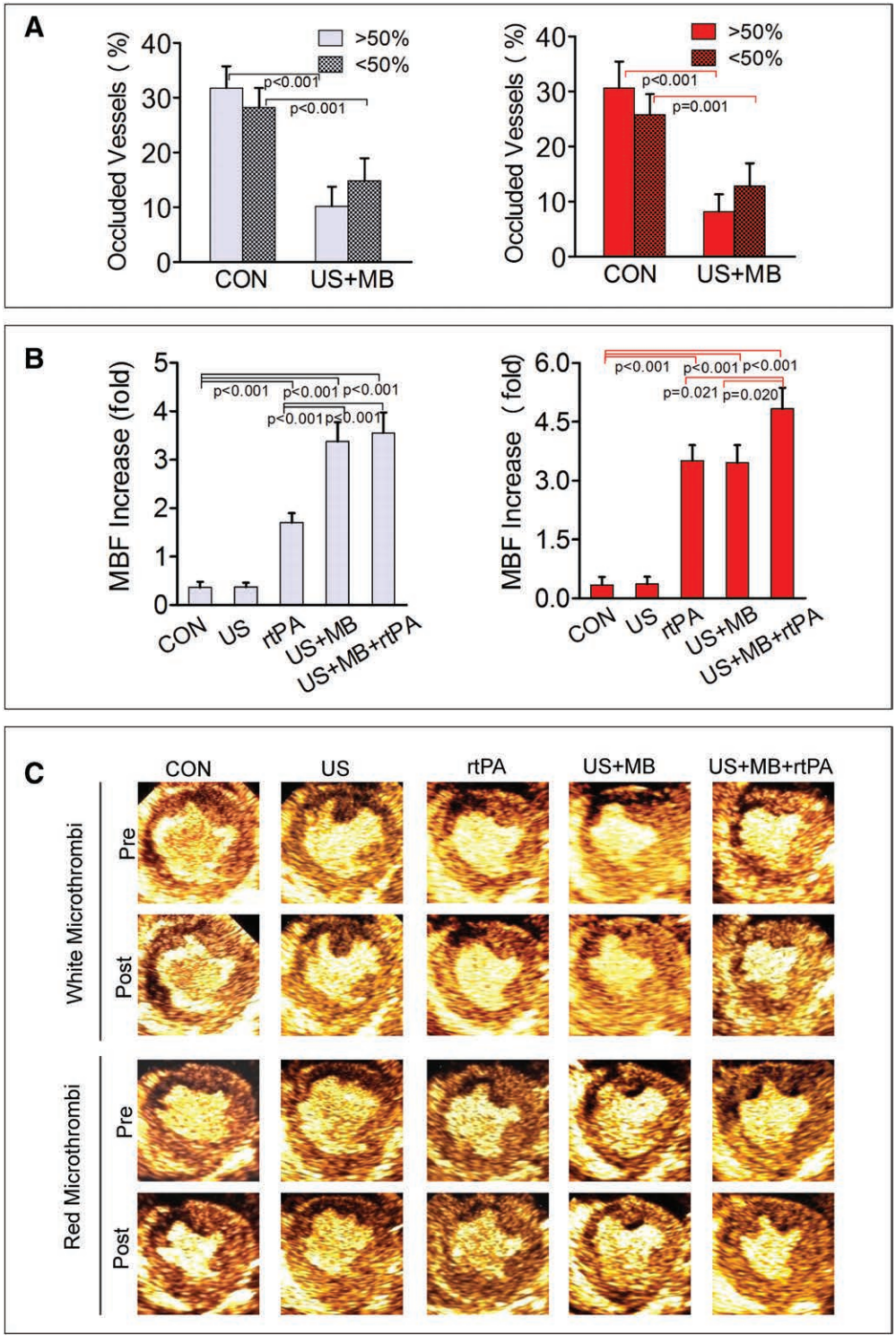

Figure 3. Effects of ultrasound (US) + microbubble (MB) treatment on microthrombi dissolution and myocardial blood flow (MBF) in canine models of coronary no-reflow. **A**, Quantification of coronary arterioles obstructed by platelet- or erythrocyte-rich microemboli (3-hr old) at 6 hr after treatment. **B**, Quantification of percentage (fold) increase of MBF as determined by myocardial contrast echocardiography (MCE) at 6 hr after treatment. **C**, Representative images of MCE (replenishment after 10 s). *White columns* refer to platelet-rich (*white*) microthrombi, whereas *red columns* refer to erythrocyte-rich (*red*) microthrombi. "⌐¬"denotes a comparison between two groups, and the corresponding *p* values are marked on the figures. $n = 5$ per group, data are shown as mean ± SD. CON = control, rtPA = recombinant tissue-type plasminogen activator, >50% = > 50% obstruction, <50% = < 50% obstruction.

$p = 0.013$) in US+MB group were larger than those in rtPA group and were comparable to US+MB+rtPA group. For ERT, the percentage increases in EF (12.08% ± 1.16% vs 8.98% ± 0.96%; $p = 0.010$) and FS (18.04% ± 0.69% vs 23.66% ± 2.15%; $p = 0.014$) in US+MB group were smaller than those in US+MB+rtPA group, and were similar in rtPA and US+MB groups.

US+MB Treatment Attenuates Myocardial Apoptosis and Inflammation

For both types of microthrombi, the percentage of apoptotic cardiomyocytes (PRT: 11.60% ± 0.35% vs 23.81% ± 0.34%, 11.23% ± 0.22% vs 23.81% ± 0.34%; ERT: 11.40% ± 0.43% vs 23.68% ± 0.31%, 5.15% ± 0.34% vs 23.68% ± 0.31%) and the number of infiltrated leukocytes (PRT: 15.83 ± 0.45/high power field [HPF] vs 32.48 ± 0.41/HPF, 15.31 ± 0.35/HPF vs 32.48 ± 0.41/HPF; ERT: 15.53 ± 0.54/HPF vs 32.28 ± 0.44/HPF, 7.26 ± 0.38/HPF vs 32.28 ± 0.44/HPF) in US+MB and US+MB+rtPA groups was lower compared with CON group ($n = 5$; $p < 0.001$), but similar in CON and US groups. For PRT, the percentage of apoptotic cardiomyocytes (11.60% ± 0.35% vs 18.61% ± 0.40%) and the number of infiltrated leukocytes (15.83 ± 0.45/HPF vs 25.37 ± 0.46/HPF) in US+MB group were lower than those in rtPA group ($n = 5$; $p < 0.001$) and were comparable to those in US+MB+rtPA group. For ERT, the percentage of apoptotic cardiomyocytes (11.40% ± 0.43% vs 5.15% ± 0.34%) and the number of infiltrated leukocytes (15.53 ± 0.54/HPF vs

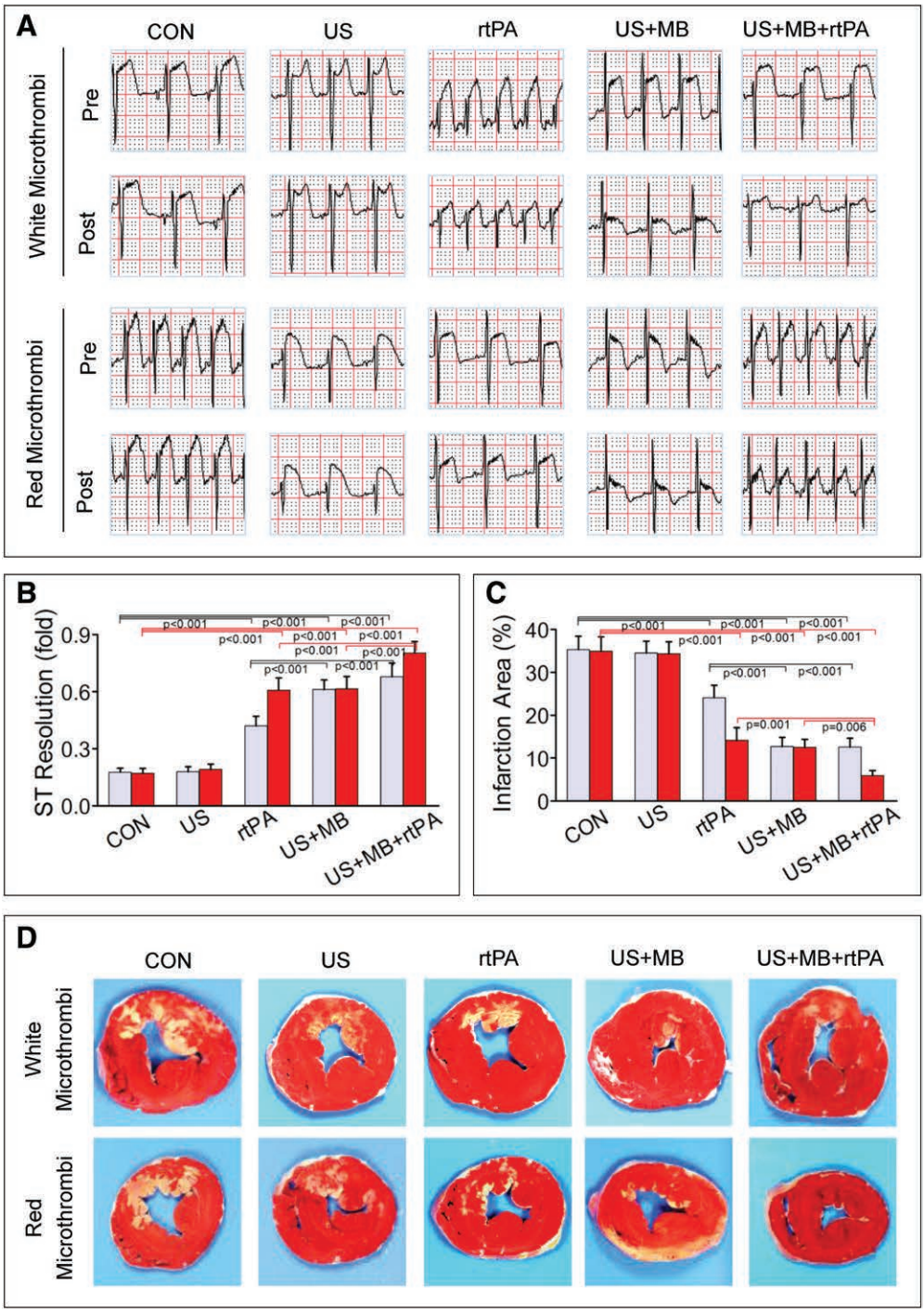

Figure 4. Effects of ultrasound (US) + microbubble (MB) treatment on ST-segment resolution (STR) and infarcted myocardial volume in canine models of coronary no-reflow. **A**, Representative electrocardiograms demonstrating ST-segment elevation both before and 6 hr after treatment. **B**, Quantification of STR at 6 hr after treatment. **C**, Quantification of 2,3,5-triphenyl-2H-tetrazolium chloride (TTC)-determined infarcted myocardial volumes at 6 hr after treatment. **D**, Representative images of slices stained by TTC at midpapillary level of canine hearts (corresponding to the second slices in each group in Fig. S9, *A* and *B*, Supplemental Digital Content 10, http://links.lww.com/CCM/D706). *White columns* for platelet-rich (*white*) microthrombi, whereas *red columns* for erythrocyte-rich (*red*) microthrombi. "⌐¬"denotes a comparison between two groups, and the corresponding *p* values are marked on the figures. $n = 5$ per group, data are shown as mean ± SD. rtPA = recombinant tissue-type plasminogen activator.

7.26% ± 0.38%) in US+MB group were higher than those in US+MB+rtPA group ($p < 0.001$), and were similar to those in rtPA group (**Fig. S10**, Supplemental Digital Content 11, http://links.lww.com/CCM/D707).

DISCUSSION

These are the major findings of this study: 1) US+MB treatment improved microvascular perfusion, attenuated myocardial injury, and preserved cardiac function in a canine model of CnRF without significant adverse effects, which could be attributed to the dissolution of coronary microthrombi by this treatment; 2) the lytic efficacy of US+MB treatment on both erythrocyte- and PRT decreased as microthrombi age increased, particularly in platelet-rich ones; and 3) for ERT, US+MB+rtPA treatment was more efficacious than US+MB in improving outcomes of CnRF.

First, the efficacy of US+MB treatment was addressed in the current study, and we found that this treatment improved myocardial perfusion in this CnRF mongrel dog model, as indicated by greater STR and an increase in MCE-measured MBF, both of which are well-established markers of microvascular perfusion (18, 26). To further explore whether this treatment ameliorated adverse outcomes by improving microvascular perfusion, the myocardial infarcted area, cardiomyocyte apoptosis, and cardiac markers (CK-MB and TnI) were evaluated by TTC staining, TUNEL staining, and ELISA, respectively. In addition, echocardiography was used to assess cardiac systolic functions (EF and FS). The results showed that US+MB treatment resulted in significant decreases in infarcted area, cardiomyocyte apoptosis, and cardiac markers, as well as dramatic increases in cardiac systolic functions, suggesting that improvements in outcomes occurred. Furthermore, the safety of US+MB treatment was also assessed, as this had been overlooked by previous studies focusing on sonothrombolysis of coronary macrothrombi.

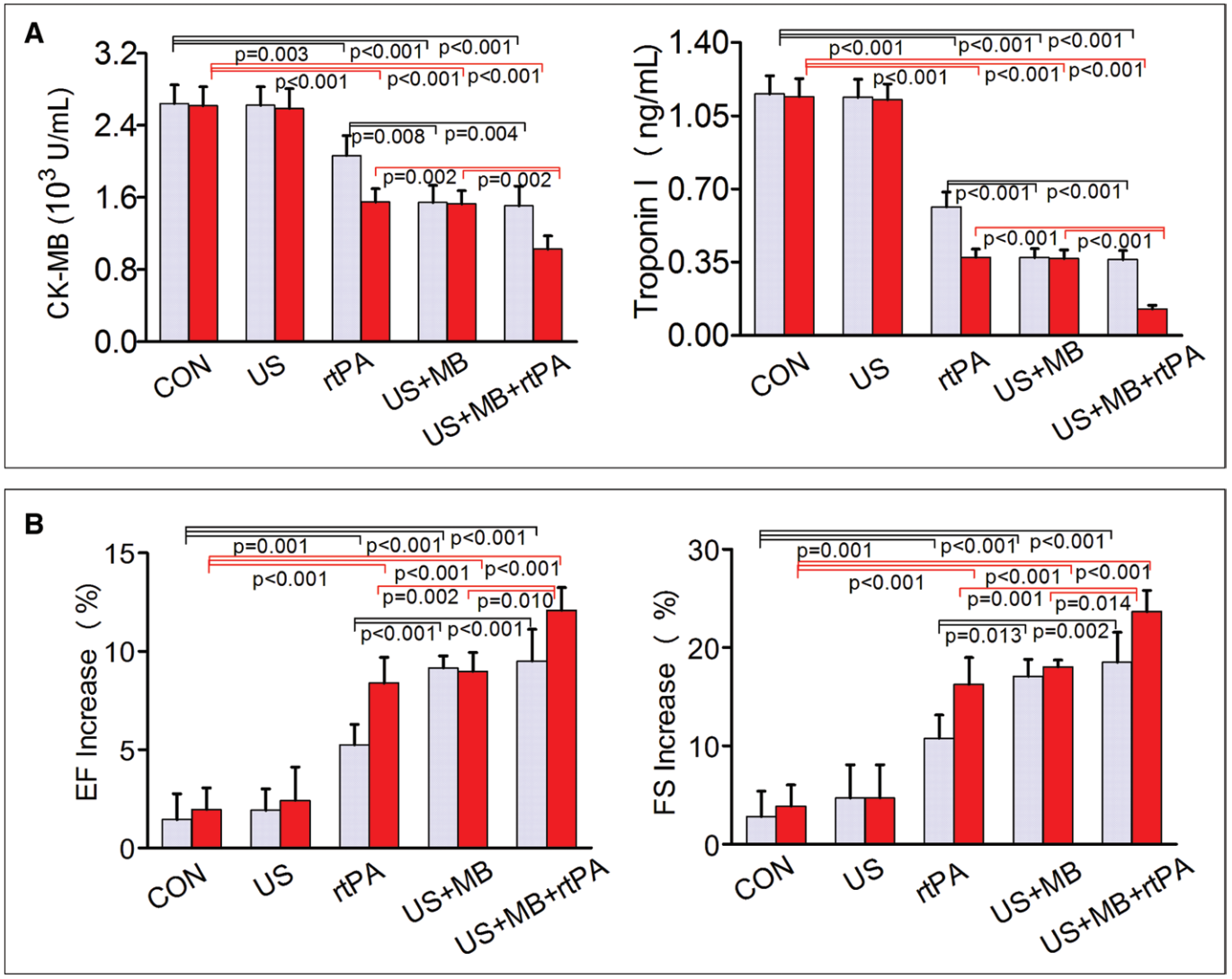

Figure 5. Effects of ultrasound (US) + microbubble (MB) treatment on cardiac markers and cardiac systolic functions in canine models of coronary no-reflow. **A**, Quantification of cardiac markers (cardiac troponin I and creatine kinase MB isoenzyme [CK-MB]) at 6 hr after treatment. **B**, Quantification of percentage increase of cardiac systolic functions (EF% = [ejection fraction (EF) after treatment – EF before treatment]/EF before treatment × 100% and FS% = [fractional shortening (FS) after treatment – FS before treatment]/FS before treatment × 100%). *White columns* denote platelet-rich (*white*) microthrombi, whereas *red columns* denote erythrocyte-rich (*red*) microthrombi. "⌐¬"denotes a comparison between two groups, and the corresponding *p* values are marked on the figures. $n = 5$ per group, data are shown as mean ± SD. CON = control, rtPA = recombinant tissue-type plasminogen activator.

Previous studies suggested that during MCE imaging with an MI of 1.3–1.5 (27, 28), continuous and prolonged US exposure along a single scan plane during MB infusion could lead to adverse effects, including ventricular premature beats and microvascular rupture. In contrast, US+MB treatment in the present study did not increase the occurrence rate of the abovementioned adverse effects, even with a higher MI (1.9); this may be ascribed to the application of multiple scan planes. Compared with continuous and prolonged US exposure along a single scan plane, multiple scan planes may dramatically lessen the energy delivered to the myocardium, thus decreasing the occurrence of adverse effects (27). Therefore, US+MB treatment could be applied to patients with acute coronary syndromes (ACSs) after receiving revascularization therapies, especially for those with a high thrombotic burden who had a great chance of developing CnRF, being a useful adjunctive strategy of revascularization therapies to improve outcomes of CnRF in ACS patients.

In the present study, the dissolution of microthrombi in mesenteric arterioles by US+MB treatment was directly visualized with an intravital microscope. Taking into consideration the close similarities of microthrombi between mesenteric arterioles and those found in coronary arterioles in terms of sizes and histologic characteristics, it can be inferred that this treatment could also effectively dissolve coronary microthrombi. More importantly, US+MB treatment decreased the percentage of microthrombi-occluded myocardial arterioles, as indicated by systemic histologic analysis of postmortem myocardium. These findings indicated that MB-mediated sonothrombolysis could efficiently dissolve coronary microthrombi, which is partially supported by previous in vivo and in vitro studies (20–22, 29). Additionally, it is widely accepted

that the burden of thrombotic microemboli is highly predictive of the occurrence of CnRF (30), and timely restoration of MBF by eliminating these emboli is the cornerstone of alleviating myocardial injury and preserving cardiac functions. Therefore, the improved outcomes in the canine CnRF models could be attributed to the dissolution of coronary microthrombi by US+MB treatment.

Both PRT and ERT are responsible for CnRF in STEMI patients (3–5). In the early stage (< 3 hr of ischemic time) of disease onset, PRT predominate, whereas in the later stage (> 6 hr of ischemic time), ERT play the leading role (31–35). Timely restoration of myocardial perfusion by dissolving microthrombi is the key to reducing cardiomyocyte death and improving CnRF. However, the currently available treatment, thrombolytics, has poor efficacy in lysing PRT (6). Interestingly, in this study, we found that US+MB treatment could lyse microthrombi and improve outcomes of CnRF much more effectively than rtPA in canine models induced by PRT, and exhibited comparable efficacy to rtPA in models induced by ERT. Our findings suggested that US+MB treatment could be a better strategy than thrombolytics for timely restoration of myocardial perfusion in CnRF by dissolving both types of microthrombi, especially in the early stage of disease onset when PRT predominate.

As indicated by HE staining and SEM, the freshly prepared platelet-rich thrombi had a relatively loose structure and more microchannels than erythrocyte-rich thrombi. As the age increased, both types of thrombi became denser and exhibited fewer microchannels, especially for platelet-rich ones, due to the fact that they were composed of more platelets than erythrocyte-rich ones, and the activation of theses platelets resulted in fibrin and clot retraction. As a result, more MBs had access to the interior of the freshly prepared platelet-rich thrombi than to erythrocyte-rich thrombi, and fewer MB had access to the interior of the older platelet-rich thrombi, as indicated by the results of contrast-enhanced US imaging, which was consistent with a previous study (36). Therefore, the lytic efficacy of US+MB treatment on both erythrocyte- and PRT decreased as microthrombi age increased, especially in platelet-rich ones. These findings suggest that US+MB treatment may be recommended for STEMI patients with microthrombi that formed within the first few hours.

There are several limitations of this study. First, outcomes were only assessed 6 hours after treatment. Although the short-term effectiveness of US+MB treatment in improving outcomes of CnRF has been proven, the long-term effectiveness is still uncertain and further experiments are needed. Second, in this study, we used the open-chest model, while in the closed-chest model, US attenuation might occur when the probe confronts the ribs and sternum over the heart, which might affect the efficacy of US+MB treatment on dissolving microthrombi. In addition, we have exclusively studied a single mechanism of no reflow, that is, microthrombi. The role of US+MB treatment in other plausible mechanisms, such as neutrophil plug or tissue edema, needs to be determined in further studies. Finally, we have only measured MBF using contrast echo, which is a well-established method to quantify MBF, combined contrast echo and microsphere method could quantify MBF more accurately.

CONCLUSIONS

US+MB treatment could improve outcomes of CnRF by lysing both erythrocyte-rich and PRT, without significant adverse effects. These findings suggest that US+MB treatment may be an effective and safe adjunctive approach for improving CnRF in STEMI patients receiving reperfusion therapy.

REFERENCES

1. Fokkema ML, Vlaar PJ, Svilaas T, et al: Incidence and clinical consequences of distal embolization on the coronary angiogram after percutaneous coronary intervention for ST-elevation myocardial infarction. *Eur Heart J* 2009; 30:908–915
2. Srinivasan M, Rihal C, Holmes DR, et al: Adjunctive thrombectomy and distal protection in primary percutaneous coronary intervention: Impact on microvascular perfusion and outcomes. *Circulation* 2009; 119:1311–1319
3. Beygui F, Collet JP, Nagaswami C, et al: Images in cardiovascular medicine. Architecture of intracoronary thrombi in ST-elevation acute myocardial infarction: Time makes the difference. *Circulation* 2006; 113:e21–e23
4. Heusch G, Kleinbongard P, Böse D, et al: Coronary microembolization: From bedside to bench and back to bedside. *Circulation* 2009; 120:1822–1836
5. Barrabés JA, Garcia-Dorado D, Mirabet M, et al: Antagonism of selectin function attenuates microvascular platelet deposition and platelet-mediated myocardial injury after transient ischemia. *J Am Coll Cardiol* 2005; 45:293–299
6. Sezer M, Okcular I, Goren T, et al: Association of haematological indices with the degree of microvascular injury in patients with acute anterior wall myocardial infarction treated with primary percutaneous coronary intervention. *Heart* 2007; 93:313–318
7. Montalescot G, Antoniucci D, Kastrati A, et al: Abciximab in primary coronary stenting of ST-elevation myocardial infarction: A European meta-analysis on individual patients' data with long-term follow-up. *Eur Heart J* 2007; 28:443–449
8. Windecker S, Kolh P, Alfonso F, et al; Authors/Task Force Members: 2014 ESC/EACTS Guidelines on myocardial revascularization: The Task Force on Myocardial Revascularization of the European Society of Cardiology (ESC) and the European Association for Cardio-Thoracic Surgery (EACTS) developed with the special contribution of the European Association of Percutaneous Cardiovascular Interventions (EAPCI). *Eur Heart J* 2014; 35:2541–2619
9. Svilaas T, Vlaar PJ, van der Horst IC, et al: Thrombus aspiration during primary percutaneous coronary intervention. *N Engl J Med* 2008; 358:557–567
10. Fröbert O, Lagerqvist B, Olivecrona GK, et al; TASTE Trial: Thrombus aspiration during ST-segment elevation myocardial infarction. *N Engl J Med* 2013; 369:1587–1597
11. Santos-Gallego CG, Vahl TP, Goliasch G, et al: Sphingosine-1-phosphate receptor agonist fingolimod increases myocardial salvage and decreases adverse postinfarction left ventricular remodeling in a porcine model of ischemia/reperfusion. *Circulation* 2016; 133:954–966
12. Mott B, Packwood W, Xie A, et al: Echocardiographic ischemic memory imaging through complement-mediated vascular adhesion of phosphatidylserine-containing microbubbles. *JACC Cardiovasc Imaging* 2016; 9:937–946
13. Hu G, Liu C, Liao Y, et al: Ultrasound molecular imaging of arterial thrombi with novel microbubbles modified by cyclic RGD in vitro and in vivo. *Thromb Haemost* 2012; 107:172–183
14. Wu J, Leong-Poi H, Bin J, et al: Efficacy of contrast-enhanced US and magnetic microbubbles targeted to vascular cell adhesion

molecule-1 for molecular imaging of atherosclerosis. *Radiology* 2011; 260:463–471

15. Wu W, Wang Y, Shen S, et al: In vivo ultrasound molecular imaging of inflammatory thrombosis in arteries with cyclic Arg-Gly-Asp-modified microbubbles targeted to glycoprotein IIb/IIIa. *Invest Radiol* 2013; 48:803–812
16. Hitchcock KE, Holland CK: Ultrasound-assisted thrombolysis for stroke therapy: Better thrombus break-up with bubbles. *Stroke* 2010; 41:S50–S53
17. Culp WC, Porter TR, McCowan TC, et al: Microbubble-augmented ultrasound declotting of thrombosed arteriovenous dialysis grafts in dogs. *J Vasc Interv Radiol* 2003; 14:343–347
18. Xie F, Lof J, Matsunaga T, et al: Diagnostic ultrasound combined with glycoprotein IIb/IIIa-targeted microbubbles improves microvascular recovery after acute coronary thrombotic occlusions. *Circulation* 2009; 119:1378–1385
19. Roos ST, Yu FT, Kamp O, et al: Sonoreperfusion therapy kinetics in whole blood using ultrasound, microbubbles and tissue plasminogen activator. *Ultrasound Med Biol* 2016; 42:3001–3009
20. Pacella JJ, Brands J, Schnatz FG, et al: Treatment of microvascular micro-embolization using microbubbles and long-tone-burst ultrasound: An in vivo study. *Ultrasound Med Biol* 2015; 41:456–464
21. Porter TR, Radio S, Lof J, et al: Diagnostic ultrasound high mechanical index impulses restore microvascular flow in peripheral arterial thromboembolism. *Ultrasound Med Biol* 2016; 42:1531–1540
22. Lu Y, Wang J, Huang R, et al: Microbubble-mediated sonothrombolysis improves outcome after thrombotic microembolism-induced acute ischemic stroke. *Stroke* 2016; 47:1344–1353
23. Mathias W Jr, Tsutsui JM, Tavares BG, et al: Diagnostic ultrasound impulses improve microvascular flow in patients with STEMI receiving intravenous microbubbles. *J Am Coll Cardiol* 2016; 67:2506–2515
24. Xie F, Gao S, Wu J, et al: Diagnostic ultrasound induced inertial cavitation to non-invasively restore coronary and microvascular flow in acute myocardial infarction. *PLoS One* 2013; 8:e69780
25. Bertuglia S: Increase in capillary perfusion following low-intensity ultrasound and microbubbles during postischemic reperfusion. *Crit Care Med* 2005; 33:2862–2864
26. Wu J, Xie F, Lof J, et al: Utilization of modified diagnostic ultrasound and microbubbles to reduce myocardial infarct size. *Heart* 2015; 101:1468–1474
27. Miller DL, Driscoll EM, Dou C, et al: Microvascular permeabilization and cardiomyocyte injury provoked by myocardial contrast echocardiography in a canine model. *J Am Coll Cardiol* 2006; 47:1464–1468
28. van Der Wouw PA, Brauns AC, Bailey SE, et al: Premature ventricular contractions during triggered imaging with ultrasound contrast. *J Am Soc Echocardiogr* 2000; 13:288–294
29. Goyal A, Yu FTH, Tenwalde MG, et al: Inertial cavitation ultrasound with microbubbles improves reperfusion efficacy when combined with tissue plasminogen activator in an in vitro model of microvascular obstruction. *Ultrasound Med Biol* 2017; 43:1391–1400
30. Otto S, Seeber M, Fujita B, et al: Microembolization and myonecrosis during elective percutaneous coronary interventions in diabetic patients: An intracoronary Doppler ultrasound study with 2-year clinical follow-up. *Basic Res Cardiol* 2012; 107:289
31. Steinvil A, Berliner S, Shapira I, et al: Time to rheology in acute myocardial infarction: Inflammation and erythrocyte aggregation as a consequence and not necessarily as precursors of the disease. *Clin Res Cardiol* 2010; 99:651–656
32. Arbel Y, Banai S, Benhorin J, et al: Erythrocyte aggregation as a cause of slow flow in patients of acute coronary syndromes. *Int J Cardiol* 2012; 154:322–327
33. Götz AK, Zahler S, Stumpf P, et al: Intracoronary formation and retention of micro aggregates of leukocytes and platelets contribute to postischemic myocardial dysfunction. *Basic Res Cardiol* 2005; 100:413–421
34. Silvain J, Collet JP, Nagaswami C, et al: Composition of coronary thrombus in acute myocardial infarction. *J Am Coll Cardiol* 2011; 57:1359–1367
35. Silvain J, Collet JP, Guedeney P, et al: Thrombus composition in sudden cardiac death from acute myocardial infarction. *Resuscitation* 2017; 113:108–114
36. Sutton JT, Ivancevich NM, Perrin SR Jr, et al: Clot retraction affects the extent of ultrasound-enhanced thrombolysis in an ex vivo porcine thrombosis model. *Ultrasound Med Biol* 2013; 39:813–824